A rock-glacier – pond system (NW Italian Alps): Soil and sediment properties, geochemistry, and trace-metal bioavailability

A rock-glacier - pond system (NW Italian Alps): soil and sediment properties, geochemistry, and trace-metal bioavailability

N. Colombo[a,b,*], C. Ferronato[c], L. Vittori Antisari[d], L. Marziali[e], F. Salerno[e], S. Fratianni[b], M. D'Amico[a], A. Ribolini[f], D. Godone[g], S. Sartini[h], L. Paro[i], U. Morra di Cella[l], M. Freppaz[a]

[a]University of Turin, Department of Agricultural, Forest and Food Sciences, Grugliasco, Italy.

[b]University of Turin, Department of Earth Sciences, Turin, Italy.

[c]Department of Veterinary Medical Sciences, University of Bologna, Bologna, Italy.

[d]Department of Agricultural and Food Sciences, University of Bologna, Bologna, Italy.

[e]CNR-IRSA (National Research Council - Water Research Institute), Brugherio, Italy.

[f]Department of Earth Sciences, University of Pisa, Pisa, Italy.

[g]CNR-IRPI (National Research Council - Research Institute for Geo-Hydrological Protection), Turin, Italy.

[h]So.Ge.T, Lucca, Italy.

[i]Arpa Piemonte, Department of "Natural and Environmental Risks", Turin, Italy.

[l]Arpa Valle d'Aosta, Department of "Climate Change", Aosta, Italy.

[*]Corresponding author: Nicola Colombo (nicola.colombo@unito.it)

Abstract

Rock-glacier sediment transfer and ice melting can impact surface waters located downstream. However, there is a lack of knowledge on the influence of rock-glacier dynamics on the geochemical, hydrochemical, and ecological characteristics of adjacent impounded surface waters. In the Col d'Olen area (Long-Term Ecological Research site, NW Italian Alps), an intact rock glacier terminates into a pond and solute-enriched waters originating from the rock glacier flow into the pond through a subsurface hydrological window. In this study, we performed geophysical and ground surface temperature measurements. Moreover, we sampled soils and sediments in different compartments of the investigated rock-glacier - pond system and we further sampled benthic invertebrates in the pond. Cold ground thermal regime, ground-ice presence, and coarse debris cover on the rock glacier together with its lithology (serpentinites) influence the rock-glacier geochemistry and ecology with respect to surrounding areas. Pond geochemistry is affected by transfer of trace-metal-enriched fine-grained debris and meltwaters from the rock glacier. Enhanced bioavailability of serpentinite-associated trace metals was proved, with concentrations of Ni and Cr in benthic invertebrates up to 384 and 110 mg kg^{-1} d.w., respectively, potentially exerting toxic effects on pond biota. The advancing movement of the rock glacier not only has delivered sediments to the pond, but it has progressively filled the valley depression where the pond is located, creating a dam that could have modified the level of impounded water. This process likely constituted a sediment trap in which serpentinitic rock-glacier sediments could be deposited at the pond bottom, with related geochemical and ecological implications. This study illustrates the importance of rock glaciers in influencing the characteristics of downstream freshwater bodies and highlights the need to improve our knowledge about climate-change-related impacts of rock-glacier dynamics on alpine headwaters.

Keywords: soil; weathering; rock glacier; lacustrine sediments; Alps; LTER

1 Introduction

Rock glaciers are slowly flowing mixtures of rock debris and ice, and constitute prominent sedimentary linkages within the alpine environment (Giardino et al., 1987). Rock glaciers act as efficient sediment conveyors in mountainous environments (Delaloye et al., 2010; Gärtner-Roer, 2012), transferring large quantities of debris from their rooting zone (upslope area) to their fronts (Kummert et al., 2018), and potentially impacting surface waters located downstream (Kummert and Delaloye, 2018a). Lakes and ponds can also form as a consequence of stream and river channel interruption due to rock-glacier advancing movement (Blöthe et al., 2019).

Melting ice in rock glaciers can impact the chemical characteristics of surface freshwater (Colombo et al., 2018a). Indeed, several studies report higher concentrations of trace metals and nutrients in their meltwaters in comparison to surface waters not affected by rock-glacier presence (Williams et al., 2006; 2007; Thies et al., 2013; Ilyashuk et al., 2014; 2018; Fegel et al., 2016; Colombo et al., 2018b; 2019). Metals in rock-glacier-affected surface waters have been also shown to bioaccumulate, potentially impacting aquatic communities (Thies et al., 2013; Ilyashuk et al., 2014; 2018).

High-elevation impounded surface waters are key freshwater reference sites for global scale processes, due to minimal direct human influence and because of their rapid response to climate-related changes (Adrian et al., 2009; Salerno et al., 2014). Recent studies have demonstrated that lakes and ponds (defined as a water bodies < 2 x 10^4 m^2, Hamerlík et al. (2014)) affected by rock-glacier ice melting have suffered changes in their chemical and biological status (Ilyashuk et al., 2014; 2018), especially in the context of climate change during the last decades (Thies et al., 2007). Recent climatic changes have caused strong modifications in glacial and permafrost environments at global scale (Harris et al., 2009; Zemp et al., 2015; Biskaborn et al., 2019) and, specifically, in the NW Italian Alps (Giaccone et al., 2015; Colombo et al. 2016a; 2016b).

Although a growing literature has documented the role of rock-glacier ice melting in impacting the alpine headwater hydrochemistry, there is a paucity of studies that investigated the influence of

rock glaciers on sedimentological, hydrochemical, and ecological dynamics of surface waters located downstream. In this context, the Col d'Olen area (NW Italian Alps) represents a suitable model system. In fact, in this area, an intact rock glacier terminates into a pond and solute-enriched waters originating from the rock glacier flow into the pond through a subsurface hydrological window (Colombo et al., 2018b; 2018c).

Our hypothesis is that the rock-glacier dynamics may influence the pond in terms of lacustrine sediment geochemistry and bioavailability of trace metals for aquatic organisms, potentially exerting adverse effects. In order to test this hypothesis, we sampled both soils and sediments in different compartments of the rock-glacier - pond system and we further sampled benthic invertebrates in the pond to: (i) assess the potential influence of the rock glacier and the surrounding soils on the lacustrine sediment geochemistry, (ii) investigate trace-metal bioaccumulation in aquatic organisms, and (iii) attempt to assess the effect of rock-glacier dynamics on potential pond systemic modifications.

2 Materials and methods

2.1 Study area

The research site is a node of the Long-Term Ecological Research (LTER) network (Angelo Mosso Scientific Institute site) in Italy, in the North-Western Italian Alps, at the boundary between Valle d'Aosta and Piemonte regions (Fig. 1a). The Col d'Olen Rock Glacier Pond is situated at an elevation of 2722 m a.s.l. and its catchment area is approximately 206,000 m^2 (Fig. 1b).

The Col d'Olen Rock Glacier can be classified as an intact bouldery, talus-tongue shaped rock glacier (cf., Haeberli et al., 2006), and it is characterised by a main flow direction from NE to SW. The rock glacier is shaped by two tongues, with one tongue (right) flowing toward a small valley depression where a pond is located, and the other one (left) flowing downstream of the pond (Fig. 1c). The rock glacier covers an area of about 37,500 m^2, while its contributing area to the pond catchment is ca. 21,800 m^2 (Fig. 1b). The fine-grained deposit constituting the interior of the rock

glacier, where outcropping, is composed by serpentinites while the surface of the landform is covered by clasts (gravel to boulders) of serpentinites and, secondarily, calcschists.

The Col d'Olen Rock Glacier Pond is situated at the rock-glacier terminus, in front of the right tongue (Fig. 1c). Its shoreline is surrounded by the rock glacier from NE to SE, with the rock-glacier front dipping into the pond. From N to SW, pedogenised slopes and a small rockfall deposit (amphibolites and calcschists) border the pond. Finally, a bare bedrock outcrop (calcschists) constitutes the southern shoreline. The pond has an area of 1,600 m^2, with a maximum depth of about 3 m, and receives rock-glacier meltwater inputs from a sub-surface hydrological window connecting the right tongue to the pond (Colombo et al., 2018c).

According to recent climate series (2008-2015) obtained by the Col d'Olen AWS (Automatic Weather Station, Meteomont Service, Italian Army, 2900 m a.s.l., 800 m far from the pond), the area is characterised by meanly 400 mm of liquid precipitation during the snow-free season, a mean annual air temperature of –2.6 °C, and a mean cumulative snowfall of 850 cm (Freppaz et al., 2019). The snowpack generally develops by late October to early November, and melt out occurs in July. The climatic classification based on the Köppen-Geiger scheme defines this area as Alpine Region, cold due to altitude (H) type (Fratianni and Acquaotta, 2017).

2.2 Ground thermal regime and rock-glacier ice content

A network of 15 temperature dataloggers was operative for 2 years (from 1 August 2014 to 31 July 2016) in the rock-glacier sediment and soil sampling areas (Fig. 1c). Ground surface temperatures (GSTs) were measured using miniature temperature loggers Maxim iButton® DS1922L (for methodological details see Gubler et al., 2011; Colombo et al., 2018b). Relevant parameters were extracted from the GST data, namely mean annual ground surface temperature (MAGST), ground freezing index (GFI), and winter equilibrium temperature (WEqT) (e.g., Delaloye, 2004; Seppi et al., 2015).

The effectiveness of geoelectrical resistivity method to detect both ground ice/permafrost and buried sedimentary ice has been largely demonstrated (e.g., Ribolini et al., 2010; Hauck, 2013). Sedimentary ice exhibits resistivity values from some MΩm to more than 100 MΩm, while pore and segregation ice (i.e., typical permafrost affected terrains) ranges between 10 kΩm to a few MΩm. Ice-debris mixtures show resistivity values varying between several hundred kΩm to about 10–20 kΩm depending on ice content and temperature, as well as mineralogical composition of rock fragments (e.g., Hauck et al., 2003; Hauck, 2013). In our study, a 2D electrical resistivity tomography (ERT) survey was performed on RG-tr to assess the presence of ice in the tongue flowing into the pond (Fig. 1c). A series of 48 electrodes were fixed into the ground along a linear profile spaced 3 m apart, and connected to a SYSCAL R1 Georesistivity Meter by means of multi-polar cables. The acquisition sequences used were the Wenner-Schlumberger and the Pole-Dipole-Dipole (Everett, 2013) (further info in Supplementary Material, Material and Methods S1). The data inversion was managed adopting a Finite Elements (FEM) 2D forward modelling algorithm. The inversion procedure used a least squares smoothness constrained approach (LaBrecque et al., 1996), with noise appropriately managed due to a data weighting algorithm (Morelli and LaBrecque, 1996). Vertical sections 15-24 m deep and 6 m wide were extracted from the complete ERT profile. The position of these sections along the profile was chosen with the aim of featuring the most relevant variations of resistivity in the subsurface.

2.3 Sampling of soils, sediments, and aquatic organisms

One 60-cm-deep soil profile was opened in the slope north of the pond (S in Fig. 1c), and the genetic soil horizons were fully described and sampled for laboratory analyses (Soil Survey Staff. 2014). The location of the soil profile was chosen because of its representativeness of the sediment deposits and parent material surrounding the pond. Indeed, soil is prevalent in the pond surroundings, excluding the rock glacier, also representing a widespread land cover in the basin (Colombo et al., 2019). Moreover, the lithology in the soil profile site is chiefly represented by amphibolites (and

calcschists), which is the prevalent lithology constituting the sediment deposits in the pond basin, thus clearly distinct from the serpentinites composing the rock-glacier interior (and secondary bedrock outcrops in the catchment). Three sediment samples were also collected for each tongue of the rock glacier at approximately 20-cm depth along the front and lateral scarps (RG-tr1–3 and RG-tl1–3 in Fig. 1c).

Two 33-cm-long lacustrine sediment cores were collected in the deepest area of the pond in September 2015 (LS1 and LS2 in Fig. 1c). A Beeker vibracore sampler (Eijkelkamp, NL) was used, equipped with a polyethylene tube with a diameter of 6 cm and a 2-m steel extension at the top of the sampler to reach the bottom of the pond. An additional 19-cm-long lacustrine sediment core was collected in the littoral part of the pond (LSa in Fig. 1c) in order to retrieve subfossil head capsules of Diptera Chironomidae and to describe ecological temporal trends of taxa assemblages.

In order to perform the analysis on trace-metal bioavailability, benthic invertebrates were qualitatively collected along two transects in the littoral part of the pond (western and southern area) using kick nets, separated according to taxon, kept in the pond water for 6 hours for gut-purging and then frozen al –20°C. Finally, lacustrine surface sediments (up to 10 cm-depth, i.e., in the uppermost sediment layer colonised by invertebrates) were collected along the two transects and used for trace-metal analysis.

2.4 Description and classification of soils

The terrestrial soil profile was classified according to the USDA Soil Taxonomy (Soil Survey Staff, 2014), as Humic Dystrochryept Coarse-loamy, Mixed. Soil samples were collected from each genetic horizon, and then divided and discussed into Soil epipedon (S-ep, A horizons, 0−18 cm depth, 2 samples) and endopedon (S-en, C horizons, 18−60 cm depth, 3 samples). Rock-glacier sediments showed no vertical stratification and similar morphological features, thus they were divided and discussed according to the flow units of the rock glacier to which they belong, i.e. Rock Glacier (RG) tongue right (RG-tr) and left (RG-tl), averaging the data obtained from the three sampling sites for

each rock-glacier tongue. Although a debate on how subaqueous substrates may be studied as soils or sediments exists (Kristensen and Rabenhorst, 2015), in order to maintain the same methodological approach in sampling and morphologically screening all the collected materials from the different system compartments, LS1 and LS2 were collected and described in the field according to the guidelines for subaqueous soils of McVey et al. (2012) and Schoeneberger et al. (2012). These morphological analyses included H_2O_2, colour change, and soil incubation test for the detection of sulphidic materials (McVey et al. 2012). The two cores were classified as Typic Haplowassent according to the USDA Soil Taxonomy (Soil Survey Staff, 2014). Samples were divided and discussed into LS epipedon (LS-ep, Ag horizons, 0−10 cm depth, 4 samples) and endopedon (LS-en, Cg horizons, 10−33 cm depth, 4 samples) (average of data obtained from the two columns).

2.5 Geochemical analyses

All soil samples were air-dried and sieved to 2 mm before analysis. Soil particle size distribution was determined by pipette method (Gee and Bauder, 1986). pH (pHmeter, Crison, Germany) and electrical conductivity (EC; conductimeter Orion, Germany) were measured on 1:2.5 (w:v) soil:deionized water suspension, while total lime ($CaCO_3$) was quantified by volumetric method (Loeppert and Suarez, 1996). Soil organic carbon (SOC) and nitrogen (SON) contents were determined by Continuous Flow-Isotope Ratio Mass Spectrometry (CF–IRMS, Delta Plus Thermo Scientific) after pre-treatment of samples with 6 M HCl at 80 °C to eliminate carbonates.

The ^{13}C abundance was expressed in delta units ($\delta^{13}C‰$):

$$\delta^{13}C‰ = [(R_{sample}/R_{standard}) - 1] \times 1000$$

where R_{sample} is the isotope ratio $^{13}C/^{12}C$ of the sample and $R_{standard}$ is the $^{13}C/^{12}C$ ratio of the Pee Dee Belemnite carbonate standard (PDB).

The $\delta^{15}N$ abundance was expressed in delta units ($\delta^{15}N‰$):

$$\delta^{15}N‰ = [(R_{sample}/R_{standard}) - 1] \times 1000$$

where R_{sample} is the isotope ratio $^{15}N/^{14}N$ of the sample and $R_{standard}$ is the $^{15}N/^{14}N$ ratio of the international atmospheric N_2 standard.

A finely ground aliquot of each sample (0.25 g) was weighed in Teflon containers and digested with aqua regia (suprapure HNO_3 and HCl 1:3, v:v, Fukla) in a microwave oven (Start D 1200, Milestone, USA) for 3 min at 250 W, 4 min at 450 W and 3 min at 700 W. After this treatment, the solution was collected in 20-ml volumetric flasks and filtered through a Watmann 42 filter. The concentration of total macro (Ca, K, Mg, P, and S) and trace metals (Cr and Ni) were recorded by Inductively Coupled Plasma Emission Spectrometer (ICP-OES, Ametek, Spectro Arcos, Germany). We considered Cr and Ni as tracers of rock-glacier influence in the pond as characteristic products from the weathering of serpentinites (e.g., Brooks, 1987).

Cr and Ni sequential extraction was performed according to Ferronato et al. (2015), with some modifications, since carbonates were absent in the samples. The extraction procedure was the following: 1) exchangeable/pH-dependent phase: 20 ml of 1M CH_3COONa (pH 5) for 5h at room temperature; 2) reducible phase: 20 ml of 0.1M NH_2OH*HCl in 25% CH_3COOH w:v (pH 2) for 16h at room temperature; 3) oxidable phase: 5ml of 30% H_2O_2 +3ml of 0.02M HNO_3 for 1h at room temperature, 2h in a water bath at 85°C (repeated twice) and finally 30 min at room temperature with 10ml of 1M CH_3COONH_4; 4) residual phase: aqua regia digestion (6ml HCl + 2ml HNO_3) with microwave oven (Millestone 1200). After each extraction, the supernatant was separated by centrifugation, while soil and sediment residue was washed twice with distilled water before the further extraction. Analyses were performed in triplicate and the trace metals extracted were analysed by ICP-OES. Soil and sediment leachability test was also performed according to Ferronato et al. (2015). Samples were shaken for 16 h with deionised water (1:10 w:v) to allow soluble elements to be extracted form soil particles and then quantified with ICP-OES.

Pearson's correlation between total Cr and Ni in all samples was calculated at a significance level of $p < 0.05$. A simple two-component mixing-analysis was performed in order to assess the relative contribution of S and RG to LS, assuming that only S and RG contribute to Ni and Cr in LS, and that

only a mixing of these two sources determines Cr and Ni concentrations in LS (cf., Haag et al., 2000; Penna and van Meerveld, 2019). The uncertainty of the model was quantified following the method of Genereux (1998). Findings of this exercise are intended to gain basic understanding of system behaviour and place bounds on potential influence of S and RG on LS, with the absolute values that have limitations due to the assumptions required for this analysis.

2.6 Aquatic invertebrate analyses

To analyse trace-metal bioaccumulation in aquatic organisms the most abundant invertebrate taxa (Diptera Chironomidae and Coleptera Dityscidae) were sorted and freeze-dried for chemical analysis. Lacustrine surface sediments were freeze-dried before chemical analyses. Invertebrates and sediments were analysed for Cr and Ni concentrations by Graphite Furnace Atomic Absorption Spectroscopy (GFAAS), after microwave assisted HNO_3 digestion. For each sample, analysis was run in duplicate and precision was better than 5%. Accuracy was estimated by analysis of reference materials BCR-278 for biota and GBW-07305 for sediments, with recoveries comprised between 75 and 102%, except for Cr in sediments, which obtained a recovery of 30%. Concentrations in sediments obtained with this weak acid extraction were considered as the fraction potentially bioavailable to sediment-dwelling organisms. Bioaccumulation of each trace metal in body tissues was expressed as Biota-Sediment Accumulation Factors (BSAF) (Wang et al., 2015), calculated as:

$$BSAF_{metal} = \frac{\text{concentration of the metal in body tissues (mg kg}^{-1}\text{ d.w.)}}{\text{concentration of the metal in sediments (mg kg}^{-1}\text{ d.w.)}}$$

For the analysis of subfossil head capsules of Diptera Chironomidae, the 19-cm-long LSa core was sectioned into layers (1–4 cm thick, according to lithological discontinuities), and 4 g of fresh sediments were deflocculated in hot KOH. Head capsules were separated under stereoscope magnification and slide mounted for taxonomic identification.

3 Results and interpretation

3.1 Thermal regime of the ground surface and ice content in the rock glacier

The thermal regimes of the ground surface show that MAGST (2.5 °C), GFI (–6 °C·day), and WEqT (0.1 °C) in the soil are far higher than on the rock glacier (Tab. 1), with values clearly indicating permafrost absence (Colombo et al., 2019). MAGST close to 0 °C, and decidedly negative GFI and WEqT confirm conditions favouring permafrost existence in the rock glacier, showing the well-known "negative thermal anomaly" characterising this coarse deposit (c.f., Harris and Pedersen, 1998), especially evident if compared to the warmer conditions characterising the soil-covered areas in the landform surroundings. On the two rock-glacier tongues MAGST is negative in RG-tr (–0.1 °C) and positive in RG-tl (0.6 °C) (Tab. 1). Also the GFI values are more negative in RG-tr (–748 °C·day) than in RG-tl (–540 °C·day). The WEqT also confirms the thermal difference between the right and the left tongue, with an average value decidedly lower in RG-tr (−4.3 °C) than in RG-tl (−3.1 °C).

The ERT results are consistent with the existence of a layer of sediments extremely rich in ice or a core of massive ice (resistivity values ranging from ca. 600−700 kΩm to 1−1.5 MΩm), at about 10 m depth and extended beneath the whole middle-upper part of RG-tr (from S3 to S8 in Fig. 2) (cf., Ribolini and Fabre, 2006; Ribolini et al., 2007; 2010). This layer coexists with frozen sediments from moderately to highly rich in ice (permafrost) (ca. 200−500 kΩm), standing on it approximately at the 5−10 m depth interval (from S3 to S7), At the very top of the ERT profile and in correspondence of the frontal scarp of the rock glacier, frozen sediments moderately to highly rich in ice characterise the subsurface below 5−6 m of depth (S2 and S8). In all examined rock-glacier sectors, the resistivity values of the shallowest layer (0−5 m, resistivity values ranging from ca. 40 to 60 kΩm) are coherent with a blocky layer, composed of large boulders (up to 2−3 metres in maximum diameter) and macropores filled by air (open-work texture) or scarce coarse gravel matrix (from S3 to S8). Frozen layers are absent in the low-resistive fine sediments composing the base of the frontal scarp (ca. 4−20 kΩm, S1) (further details in Supplementary Material, Results S2).

3.2 Morphological, physicochemical, and geochemical properties

The physicochemical features of all soil and sediment samples are shown in Table 2. Low clay content is detected in all samples (4−11%). RG sediments are characterised by higher sand content (76−79%) than LS and S samples, while silt component is predominant in LS (77−83%). From a textural point of view, RG, LS, and S samples can thus be considered loamy sand, silty loam, and medium loam, respectively. pH values decrease from RG samples (6.7−6.6) to LS (5.2) and S (4.9−5.1) (Tab. 2). It is worth noting that LS shows a definitively higher EC (347−369 µS cm^{-1}) with respect to the values found in RG and S.

In RG samples very low SOC concentrations are detected (0.3−0.4 g kg^{-1}) (Tab. 2), while higher values are found in LS and S. SOC distribution along the LS profiles shows a C enrichment in the deeper horizons (2 g kg^{-1}). Remarkably, the opposite trend is noted in S, where C drastically decreases from S-ep to S-en (1.3 g kg^{-1}). Differences in stable isotopic signature among the samples are displayed in Fig. 3. The negativity of $\delta^{13}C$ increases from RG-tr to LS and S, while the opposite trend is detected for $\delta^{15}N$ (S to LS and RG) (Tab. 2).

3.3 Major elements and trace metals

Table 3 shows the mean major elements and trace metals distribution in the different selected compartments of the study area (RG, LS, and S). S shows a different composition with respect to RG. S is enriched in nutrients (e.g., Ca, K, and P), while Cr and Ni are up to 10 times lower in S than in RG. Considering the distribution of elements along the sediment profiles, S and LS show an opposite pattern: some macronutrients (e.g., Ca, K, and P) decrease from top to deep S layers, while the opposite trend is found in LS. Cr and Ni correlation in all samples is significantly positive ($r = 0.94$), with LS highlighting a more similar Ni and Cr content to RG than S (Fig. 4). A simple two-component mixing-analysis was performed and the results show that the relative contributions of Cr and Ni of RG to LS are 62±22% and 63±18%, respectively.

The sequential extraction results of Cr and Ni in RG, LS, and S samples are shown in Fig. 5. As expected, RG shows the highest Cr and Ni content. In both tongues, Cr is almost totally found in the residual phase, while Ni is highly available as reducible forms (36 and 28% in RG-tr and RG-tl, respectively). In addiction RG-tr also shows a 13% exchangeable Ni. Similarly, in LS Cr is almost completely immobilised in the residual fraction (accounting for ca. 95%) although a slightly greater availability is shown in comparison to RG, while Ni shows greater availability (38% in LS-ep and 50% in LS-en) with respect to Cr. Again, LS shows more similar contents to RG than S. Very low total amount of both metals is found in S. The availability of Cr (below 8%) and Ni (below 16%) in S is low, although a slightly greater Cr availability is found with respect to the other sampling sites, especially RG. To further deepen the comparison among the analysed environmental compartments, soluble elements extracted from soil and sediment are shown (Tab. 4). Notably, soluble Ca, Mg, S, and Ni are up to one order of magnitude more soluble in LS than in S and RG.

3.4 Aquatic organisms

Benthic community analysis shows that the pond is colonised mainly by Diptera Chironomidae (dominated by the species *Paratanytarsus austriacus*), Coleoptera Dytiscidae (*Agabus* sp. and *Potamonectes* sp.), Trichoptera Limnephilidae, and Oligochaeta Tubificidae.

Bioaccumulation in invertebrates shows the highest concentrations for Ni, with values of 345.9 ± 54.2 mg kg^{-1} d.w. in Chironomidae (sediment-dwelling organisms; *P. austriacus* is a sediment-feeder; e.g. Moog et al., 2005) and 20.8 ± 2.8 mg kg^{-1} d.w. in Dytiscidae (predators of benthic organisms; e.g., freshwaterecology.info) (Fig. 6a). Cr shows a concentration of 106.0 ± 6.1 mg kg^{-1} d.w. in Chironomidae, followed by Coleoptera (5.4 ± 3.5 mg kg^{-1} d.w.). Concerning the sediments, the uppermost layer colonised by benthic organisms shows Ni values up to 486 mg kg^{-1} d.w. and Cr concentrations up to 196 mg kg^{-1} d.w.

According to BSAF calculation, Chironomidae show significant bioaccumulation from sediments (BSAFs between 0.6 and 1.3), while values in Coleoptera are very low (BSAFs ≤ 0.05), showing

other potential exposure pathways (Fig. 6b). Moreover, the most bioavailable metals is Ni, with BSAF values of almost 1 for Chironomidae. On the contrary, Cr shows BSAF values for Chironomidae around 0.6, showing lower availability for sediment-dwelling organisms.

To analyse potential paleo-ecological changes in Chironomidae assemblages, subfossil head capsules were analysed in the LSa core. Head capsules are present only in the most recent sections, from 6.5-cm depth to the column top. Therefore, a taxonomical analysis is not further performed.

4 Discussion

Despite the increasing interest on the effects of rock-glacier ice melting, a lack of knowledge exists about the influence of rock-glacier sediment transfer and hydrochemical dynamics on the geochemical and ecological characteristics of a connected hydrological system. By analysing the physiochemical, geochemical, and ecological conditions of the rock glacier and of the surrounding lacustrine and terrestrial soil, we attempt to highlight the main differences and the possible connections among the different compartments, in order to assess the effect of the rock-glacier dynamics on the system characteristics and potential systemic modifications.

4.1 Physiochemical, isotopic and geochemical differences among compartments

The physicochemical analysis of the different RG, LS, and S compartments reveals that the system is generally characterised by a sub-acidic environment, with pH values that decrease from 6 to 5 from RG to S. In this context, SOC is rather low, especially in RG, which shows a content below 0.5 g kg^{-1}, thus highlighting a very mineral and non-vegetated environment. The analysis of the isotopic signature of the samples well describes the different environmental conditions that characterise the compartments of the studied setting. The $\delta^{13}C$ values in S are in the range of values reported for high-elevation soils (Bird et al., 1994), while in LS and RG are less negative and out of the range reported for high-elevation soils by Körner (2003). Our data of $\delta^{13}C$ and $\delta^{15}N$ highlight that S is characterised by the typical signature of C3 plants (Bristow et al., 2013), while in LS and RG less negative $\delta^{13}C$

values and low $\delta^{15}N$ ones suggest the presence of aquatic primary producers (e.g., algae) and lichens (White, 2015). The C/N ratio at LS-ep and LS-en (ca. 10) reveals a mixture of algal and higher plant material (Wang and Wooller, 2006; Fan et al., 2017), while the $\delta^{13}C$ values higher than -26‰ seem to exclude the presence of phytoplankton (Wang and Wooller, 2006).

The isotopic difference between the rock glacier and the surrounding areas shows the uniqueness of the rock-glacier environment, characterised by cold ground thermal regimes typical of permafrost conditions, surface movements, and presence of coarse debris cover (Harris and Pedersen, 1998; Hoelzle et al., 1999; Haeberli et al., 2006), that can deeply influence its ecology in comparison to surrounding areas (Tampucci et al., 2017). Indeed, while the soil sampling site was characterised by the distributed presence of vegetal species (*Cirsium spinosissimum*, *Geum montanum*, *Campanula scheuchzeri*, *Ranunculus acris*, *Lotus corniculatus subsp. alpinus*, *Festuca varia*, *Veronica alpina*, *Sempervivum arachnoideum*, and *Carex curvula*), plant cover is extremely reduced on the rock-glacier surface (patchy presence of endemic species *Cardamine plumieri*, *Thlaspi sylvium*, and *Rhodiola rodea*), probably due to the widespread presence of a coarse debris cover, which is known to be a fundamental factor limiting plant colonisation on rock glaciers (Gobbi et al., 2014; Colombo et al., 2016a). Another factor influencing the vegetation development on the rock glacier could be the serpentinitic lithology composing the fine-grain sediments in the rock-glacier interior. Indeed, although some vegetation cover has been previously found on lateral and terminal zones of intact rock-glacier tongues where finer detritic rock material occurs (Burga et al., 2004; Colombo et al., 2016), plant colonisation on serpentinitic materials should be particularly difficult because of the low amount of available nutrients and high concentrations of phytotoxic elements (e.g., Ni) (D'Amico et al., 2017). Thus, although several rock glaciers have been reported to host vascular plants (Cannone and Gerdol, 2003; Burga et al., 2004), the isotopic values are in agreement with the observed general lack of vegetation colonisation on the rock-glacier surface. Finally, although no specific investigation was performed in order to determine the presence and characteristics of lichens on the rock-glacier body, their presence has been reported on other rock glaciers with different activity stages (Cannone

and Gerdol, 2003; Burga et al., 2004), hence the isotopic data indicating the presence of lichens at the RG sampling sites seem reasonable.

RG-tr shows differences in $\delta^{13}C$ in comparison to RG-tl. It is possible to assume that the colder ground thermal regime and the presence of high internal ice content in RG-tr are capable to differentiate the ecological characteristics of the two tongues. The less negative $\delta^{13}C$ in the right tongue can be attributed to the low temperature-induced organic matter decay. High moisture and low temperature are capable to slow down the decomposing activities of microbes and this may have led to accumulation of more less-decomposed organic matter in sediments (Du et al., 2014). These differences are also well represented by the surface morphology, with RG-tr showing well evident surface flow features (ridges and depressions), high steepness of the front and a general turgid shape. Differently, the surface micro-topography of the left tongue is relatively subdued with respect to the right one, suggesting lower ice content (c.f., Haeberli et al., 2006; Jones et al., 2018).

Different geochemical features are also present in the chemical speciation of the two key metals that characterise the system, Cr and Ni. Indeed, RG-tr shows higher Cr and Ni content with respect to RG-tl, with the former displaying higher Ni availability. Enhanced mechanical alteration and greater availability of water in RG-tr might increase weathering processes (c.f., Kandji et al., 2017; Colombo et al., 2019), resulting in higher trace-metal content and higher mobility of Ni with respect to RG-tl. This mechanical alteration, together with transport processes (discussed below) is reflected in both LS-ep and LS-en, where the exchangeable Ni fraction increases of meanly 10%, while in S most of the Ni is in the residual fraction. Regarding Cr, its generally lower mobility compared to Ni in serpentine soils and sediments has been largely reported in literature (Hseu et al., 2018 and references therein reported), thus explaining the pattern found in RG samples. The increasing percentage of Cr in the reducible phase of LS and S samples could be due to autochthonous mobilisation processes that may be linked to both abiotic or biotic pedogenetic (e.g., production of organic acids from the soil organic matter) processes (Mandal et al., 2011; Löv et al., 2017).

4.2 Rock-glacier influence on pond geochemistry

The decreasing concentration of key serpentinitic trace metals from RG to LS and S, with RG and LS displaying more similar contents, confirms the decisive influence of the rock glacier on the geochemical characteristics of the lacustrine sediments in the pond. Indeed, although serpentinites are also present in the rock-glacier catchment as secondary bedrock outcrops, the majority of the debris deposits in the catchment are composed by amphibolites (and minor calcschists and paraschists), thus showing a similar lithology characterising the areas around the pond (Colombo et al., 2019), hence explaining the different content of Cr and Ni in S. Moreover, although rock glaciers are chiefly considered one of the main storage components of the coarse debris system in mountainous environments (Barsch and Caine, 1984), the amount of fine-grained material in the rock-glacier interior can be relevant (Haeberli et al., 2006), as also observed in the frontal and lateral scarps of the Col d'Olen Rock Glacier. Thus, since the rock glacier offers a proportion of mobile (serpentinitic) fine-grained material (Kummert and Delaloye, 2018a) far higher than the surrounding vegetated soils, undergoing slower rates of erosion (Stanchi et al., 2015), and other bedrock and coarse debris deposits, the accumulation of such material at the bottom of the pond in which RG-tr terminates is likely enhanced. This is in agreement with our data, that show a higher percentage of fine material (e.g., silt) at the bottom of LS with respect to RG. Silt is among the most erodible size classes in soils (Wischmeier and Mannering, 1969) and extremely limited organic matter content in RG likely enhances sediment erodibility, with the erosion rate that is probably exacerbated by the steep slope of the frontal and lateral scarps of the landform.

A combination of factors responsible for sediment transfer from rock glaciers have been reported in literature. Previous studies described rock-glacier outflows as clear (i.e., predominantly sediment free), containing comparatively lower suspended sediment concentrations with respect to glacier-fed outflows (Gardner and Bajewsky, 1987), pointing to a potential filtering effect of rock glaciers on fine-grained sediment throughput (Jones et al., 2019). However, other studies reported increasing suspended sediment loads for rock glaciers at peak discharges (Krainer and Mostler, 2002), in

response to precipitation events (Gardner and Bajewsky, 1987). Colombo et al. (2018c) reported higher estimated rock-glacier discharges after precipitation events, thus increasing sediment contributions might occur during discharge peaks, although the relationship between discharge and sediment export from rock glaciers is still unclear (Jones et al., 2019). However, considering that RG-tr terminates into the pond, direct sediment transfer from the rock glacier to the pond is likely to be predominant. Indeed, Kummert et al. (2018) individuated multiple erosion processes at the front of rock glaciers responsible for sediment transfer (from boulders to fine sediments) from the landforms to downslope zones due to rock-glacier advance and water inputs. Thus, the advancing movement of the rock glacier with the material transported towards and down the rock-glacier front (cf., Kääb and Reichmuth, 2005) together with potential debris slides and superficial flow events affecting larger areas on the frontal slope occurring when water is added (cf., Kummert et al., 2018) are likely the main processes contributing to rock-glacier-originated sediment accumulation at the pond bottom.

The rock-glacier influence on the lacustrine sediment geochemistry can also be seen as an important factor acting as a trigger for autochthonous processes that characterise the subaqueous pedogenesis in the pond. It is well consolidated that soils develop at contact of earth surface with air however, in the last decades, researchers have demonstrated that soil can develop also under submerged conditions. In these conditions, some pedogenetic processes may occur similar to terrestrial environment, thus developing proper subaqueous pedons (Demas and Rabenhorst, 1999; 2001; Erich et al., 2010). These findings have been internationally recognised by different international classification systems (Demas and Rabenhorst, 1999; Soil Survey Staff, 2014; IUSS 2015), and today these guidelines support and incentivise the attempt to study the subaqueous environment from a pedological point of view, in order to implement data collection and definition of specific diagnostic properties of subaqueous pedons. The study of subaqueous pedogenesis, in fact, is relatively recent and in high-mountain systems is still largely unknown. In our view, the physical transfer of fine material from the rock glacier to the pond in the investigated system may represent an important trigger for this pedogenesis. This in in agreement with the findings of Mania et al. (2019),

who discovered analogies in bacterial communities structure and composition between pond and RG-tr sediments, attributing this evidence to an enhanced fine-grain sediment contribution from the rock glacier to the pond. If biological modifications of submerged sediments occur based on the presence of fine-grain materials, we could hypothesise that the increase of silt component in LS, associated to a change of the microbial structure and metabolism and with the occurrence of intra-pond weathering processes, could be responsible of the increase of EC and the consequent increase of soluble nutrients (e.g., Ca and Mg) and trace metals (e.g., soluble Ni from geogenic rock-glacier material).

Another effect of rock-glacier dynamics into the pond is associated with the "leaching" effect of soluble elements, such as Ni. From a purely water-chemistry standpoint, Colombo et al. (2018b; 2019) reported Ni concentrations (mean: 35 μg L^{-1}) at the sub-surface hydrological window connecting RG-tr to the pond, during estimated rock-glacier discharge peaks (Colombo et al., 2018c), to be approx. 7 times higher than the ones measured at two transient springs (present only during snowmelt and heavy rainfall periods, mean: 5 μg L^{-1}, unpublished data) in the catchment during the ice-free (pond without ice cover) seasons 2014 and 2015. Generally, the mobility of Ni is higher at lower pH (Kandji et al., 2017). In RG sediments pH is below 7 while in the rock-glacier meltwater pH is below 8 (Colombo et al., 2018b; 2019), thus part of the dissolved Ni was found in water solution, while at higher pH (>8) it would have been completely precipitated (Kandji et al., 2017). This evidence further supports the role of the rock glacier in exporting serpentine-derived products in the pond, also in terms of dissolved chemical species, with potentially important consequences for aquatic communities in the pond.

4.3 Rock-glacier influence on trace-metal bioavailability

A further evidence of the relevant rock-glacier influence on the pond geochemical and ecological dynamics was obtained by the analyses of benthic invertebrates. Concentrations of key trace metals in sediments and aquatic organisms can be compared to another rock-glacier - pond system in the Alps studied by Ilyashuk et al. (2014). Values in our samples are even higher both for sediments and

biota, confirming the key role of rock glaciers in determining the chemical characteristics of pond ecosystem. From an ecotoxicological point of view, the most striking evidence is Ni concentration in lacustrine surface sediments, which are ten times higher than values considered toxic for benthic organisms, e.g., the consensus based-Probable Effect Concentration (cb-PEC) of 48.6 mg kg^{-1} d.w. (MacDonald et al., 2000). As well, Cr values were above the corresponding cb-PEC of 111 mg kg^{-1} d.w. However, toxicity is strictly bound to bioavailability of the metals. Results of sequential extraction and of bioaccumulation in benthic organisms confirm enhanced bioavailability in the aquatic environment. This could be related to high concentrations of trace metals in the dissolved and particulate phase, as also expected in the rock-glacier meltwater (Colombo et al., 2018b; 2019) and in general in other rock-glaciated settings (Ilyashuk et al., 2014; 2018).

As obtained by Ilyashuk et al. (2014), Chironomidae show higher concentrations than Coleoptera. This may be related to different uptake/excretion efficiency of the organisms (Rainbow, 2002) but also to different exposure routes (Goodyear and McNeill, 1999; Lee et al., 2000). Chironomidae, dominated by the sediment-feeder *P. austriacus*, may be exposed mainly by ingestion of contaminated sediments and porewater. The predators Coleoptera Dytiscidae may accumulate mainly by ingestion of contaminated preys or directly from the water. It has been demonstrated that most metals show biodilution in aquatic food chains, with lower values at higher levels of the trophic chains in comparison to basal levels (Watanabe et al., 2008). This may explain the lower values obtained for Coleoptera in comparison to Chironomidae. However, both taxa show Ni concentrations higher than invertebrate body burdens considered as thresholds above which benthic communities show alterations due to metal contamination (6.5 mg kg^{-1} d.w. for Ni according to Bervoets et al. (2016)). As well, Chironomidae show Cr concentrations above the threshold of 10 mg kg^{-1} d.w. (Bervoets et al., 2016). For this latter metal, bioavailability was proved to be lower in comparison to Ni, showing the lowest BSAF value for both taxa. This is in agreement with results of sequential extraction, which prove a low availability for this metal.

4.4 Potential links between rock-glacier dynamics and pond systemic modifications

Contrary to what observed in the soil, the concentrations of organic C and other nutrients and macroelements (e.g., Ca, K, P, and S) in the lacustrine sediments increase in the endopedon. These elements are generally associated with biological contribution from mineral soils, also considering the very low concentration of the same elements in the rock glacier. In addition, head capsules of Chironomidae were found only in the most recent lacustrine sediment layers of the core collected in the littoral area. This result suggests that the pond water surface in the past was likely not as extended as it has been in the most recent period. It is even possible that part of the current pond was interested by the presence of a swamp in the past thus explaining the increase in soil-derived elements in the endopedon, although further in-depth investigations are required to substantiate this speculation. However, these findings are in agreement with the assumptions proposed by Colombo et al. (2018c). Indeed, these authors assumed that the rock-glacier advance has progressively filled the valley depression where the pond is located, creating a dam that could have modified the level of impounded water. Differently, the slight decrease in $\delta^{13}C$ in LS-ep may have been the result of a more recent increase in the relative contribution of isotopically-lighter, terrestrial organic matter (Talbot and Lærdal, 2000; Fan et al., 2017) related to the development of a vegetated landscape in the basin (c.f., Thevenon et al., 2012). A similar pattern can be seen for $\delta^{15}N$, and this may have been related to the effect of inputs of isotopically-lighter soil nitrogen on the dissolved inorganic nitrogen pool in the pond (Peterson and Howarth, 1987; Fan et al., 2017). However, slightly lower $\delta^{13}C$ and $\delta^{15}N$ in LS-ep could be also explained by increased dissolved CO_2 supply to the pond water owing to a reduction in the seasonal ice cover (enhanced exchange between the atmosphere and the pond water) or changes in the pond trophic levels (Harwart et al., 1999; Teranes and Bernasconi, 2005).

Only recently, researchers have explored whether and how rock glaciers influence mountainous hydrological systems by advancing onto valley floors, and physically disrupting water and sediment fluxes, forming lakes, backwater sediment wedges, and constricting channels (Blöthe et al., 2019). Indeed, when connected to channels, periglacial moving landforms can represent substantial active

sources of sediments (Kummert and Delaloye, 2018b). Erosion rates responsible for sediment removal are then influenced by the erosion susceptibility of the sediments lying at the fronts, as well as water availability in the downstream zones. In the case of the Col d'Olen Rock Glacier, the advancing movement of the rock glacier has likely modified the configuration of the valley depression, which has been progressively filled by the rock glacier (Colombo et al., 2018c). In turn, this likely constituted a sediment trap in which fine serpentinitic sediments mainly originated from the rock glacier could be deposited at the bottom of the pond, with related geochemical and ecological implications. Although prior studies (e.g., Evin, 1987) and reviews (e.g., Haeberli et al., 2006) affirmed that rock glaciers would be comparatively rare in weak rocks that disintegrate into fine and platy debris, such as schists, serpentinites and their tendency to weather can be relevant for rock-glacier formation (Scotti et al., 2013). Moreover, considering that several rock glaciers have accelerated considerably in recent decades due to climate change in different mountain ranges (e.g., Delaloye et al., 2010; Daanen et al., 2012; Sorg et al., 2015), the availability of unconsolidated sediments downslope may increase substantially, potentially affecting the sediment transfer rates (Kummert et al., 2018) into downstream water bodies. Thus, the geochemical and ecological impacts reported in this study could be relevant at wider scale. However, it is important to consider that in our study we did not investigate the geochemical and ecological conditions downstream the pond, since the pond has no surface outflow. Thus, this occurrence together with the potential changes in rock-glacier effluent hydrochemistry within a few hundreds of metres downstream (c.f., Thies et al., 2018) prevent extending our considerations further downstream the investigated system.

Finally, considering the high range of sedimentation rates in similar rock-glaciated environments (from ca. 0.01 to 0.07 cm yr^{-1}, Ilyashuk et al. (2014) and Putnam and Putnam (2009), respectively), our LS could cover from ca. 470 to 3,300 years. Thus, great uncertainty exists about the environmental modifications that took place in the catchment and the pond, and when they occurred. At this regards, performing more comprehensive lacustrine records, encompassing sediment dating, could help to inform our understanding of the pond temporal evolution and to improve our ability to infer the effects

of past changes in rock-glacier dynamics on the hydrochemical, geochemical, and ecological characteristics of the investigated rock-glacier - pond system.

Conclusion

In this study we show that the unique characteristics of the rock-glacier environment (i.e., cold ground thermal regimes, ground-ice presence, and coarse debris cover) and its lithology (serpentinites) influence the rock-glacier geochemistry and ecology in comparison to surrounding areas. Fine-grained sediment transfer from the rock glacier to the pond is probably the most important process affecting the geochemistry of lacustrine sediments. It is likely that the rock-glacier advance has progressively filled the valley depression where the pond is located, creating a dam that could have modified the level of impounded water; in turn, this constituted a sediment trap in which serpentinitic rock-glacier sediments could be deposited at the pond bottom, with related geochemical and ecological implications. Moreover, the export of trace-metal-enriched sediments and meltwaters from the rock glacier into the pond determines enhanced bioavailability of Ni and Cr for aquatic organisms. This implies that resident communities may have developed high resistance to trace metals, which could be investigated in comparison to nearby ponds not influenced by the rock glacier. In this study we showed the effects of rock-glacier dynamics on the characteristics of downstream surface waters, highlighting the need to improve our knowledge about rock-glacier-related impacts on high-elevation headwaters in the context of climate change.

Acknowledgments

We would like to thank Gaetano Viviano, Cristina Viani, Marco Bacenetti, Gioachino Roberti, Ilaria Mania, Roberta Gorra and Elena Serra for their help in field work activities. We are also grateful for the support given by Daniele Bormioli, Giuseppina Moletta and Giacomo Refiorentin (Arpa Piemonte), and Marco Giardino, Luigi Perotti, Lino Judica and Adriana Bovio (University of Turin). We give special thanks to the family Beck-Peccoz, Consorzio di Miglioramento Fondiario di

Gressoney (Aosta) and MonteRosa-ski for allowing the access to the study site. This research has been partially developed in the framework of the PRIN 2010-11 (funded project of the Italian Ministry for Education and Research) named “Response of morphoclimatic system dynamics to global changes and related geomorphological hazards” (coord. Prof. Carlo Baroni), the European Regional Development Fund in Interreg Alpine Space project Links4Soils (ASP399): Caring for Soil-Where Our Roots Grow (http://www.alpinespace.eu/projects/links4soils), and ARPA Piemonte funds provided to the University of Pisa (P.I. Adriano Ribolini).

Reference list

Adrian, R., et al., 2009. Lakes as sentinels of climate change. Limnology and Oceanography 54(6), 2283–2297. https://doi.org/10.4319/lo.2009.54.6_part_2.2283

Barsch, D., Caine, N., 1984. The nature of mountain geomorphology. Mountain Research and Development 4, 287–298. doi:10.2307/3673231

Bervoets, L., et al., 2016. Identification of threshold body burdens of metals for the protection of the aquatic ecological status using two benthic invertebrates. Environmental Pollution 210, 76–84. https://doi.org/10.1016/j.envpol.2015.12.005

Bird, M.I., et al., 1994. Effect of altitude on the carbon-isotope composition of forest and grassland soils from Papua New Guinea. Global Biogeochemical Cycles 8(1), 13–22. https://doi.org/10.1029/93GB03487

Biskaborn, B.K., et al., 2019. Permafrost is warming at a global scale. Nature Communications 10, 264. https://doi.org/10.1038/s41467-018-08240-4

Blöthe, J.H., et al., 2019. Rock-glacier dams in High Asia. Earth Surface Processes and Landforms 44, 808–824. https://doi.org/10.1002/esp.4532

Bristow, L.A., et al., 2013. Tracing estuarine organic matter sources into the southern North Sea using C and N isotopic signatures. Biogeochemistry 113, 9–22. https://doi.org/10.1007/s10533-012-9758-4

Brooks, R.R., 1987. Serpentine and its vegetation. A multidisciplinary approach. Ecology, Phytogeography, and Physiology series. Dioscorides Press, Portland.

Burga, C.A., et al., 2004, Vegetation on Alpine active rock glaciers surfaces: a contribution to abundance and dynamics on extreme plant habitats. Flora 199, 505–515. https://doi.org/10.1078/0367-2530-00179

Cannone, N., Gerdol, R., 2003. Vegetation as an ecological indicator of surface instability in active rock glaciers. Arctic, Antarctic and Alpine Research 35, 384–390. https://doi.org/10.1657/1523-0430(2003)035[0384:VAAEIO]2.0.CO;2

Colombo, N., et al., 2016a. Recent transition from glacial to periglacial environment in a high altitude alpine basin (Sabbione basin, north-western Italian Alps). Preliminary outcomes from a multidisciplinary approach. Geografia Fisica e Dinamica Quaternaria 39(1), 21–36. doi 10.4461/GFDQ.2016.39.3

Colombo, N., et al., 2016b. Geomorphology of the Hohsand basin (Western Italian Alps). Journal of Maps 12(5), 975–978. https://doi.org/10.1080/17445647.2015.1105762

Colombo, N., et al., 2018a. Review: Impacts of permafrost degradation on inorganic chemistry of surface fresh water. Global and Planetary Change 162, 69–83. https://doi.org/10.1016/j.gloplacha.2017.11.017

Colombo, N., et al., 2018b. Rainfall as primary driver of discharge and solute export from rock glaciers: the Col d'Olen rock glacier in the NW Italian Alps. Science of the Total Environment 639, 316–330. https://doi.org/10.1016/j.scitotenv.2018.05.098

Colombo, N., et al., 2018c. Mechanisms linking active rock glaciers and impounded surface water formation in high-mountain areas. Earth Surface Processes and Landforms 43(2), 417–431. https://doi.org/10.1002/esp.4257

Colombo, N., et al., 2019. Influence of permafrost, rock and ice glaciers on chemistry of high-elevation ponds (NW Italian Alps). Science of the Total Environment 685, 886–901. https://doi.org/10.1016/j.scitotenv.2019.06.233

Daanen, R.P., et al., 2012. Rapid movement of frozen debris-lobes: implications for permafrost degradation and slope instability in the south-central Brooks Range, Alaska. Natural Hazards and Earth System Sciences 12(5), 1521–1537. https://doi.org/10.5194/nhess-12-1521-2012

D'Amico, M.E., et al., 2017. Primary vegetation succession and the serpentine syndrome: the proglacial area of the Verra Grande glacier, North-Western Italian Alps. Plant and Soil 415, 283–298. https://doi.org/10.1007/s11104-016-3165-x

Delaloye, R., 2004. Contribution à l'étude du pergélisol de montagne en zone marginal. PhD Thesis, GeoFocus 10, Département de Géosciences, Université de Fribourg.

Delaloye, R., et al., 2010. Overview of rock glacier kinematics research in the Swiss Alps. Seasonal rythm, interannual variations and trends over several decades. Geographica Helvetica 65(2), 135–145. https://doi.org/10.5194/gh-65-135-2010

Demas, G.P., Rabenhorst, M.C., 1999. Subaqueous soils: pedogenesis in a submersed environment. Soil Science Society of America Journal 63, 1250–1257. https://doi.org/10.2136/sssaj1999.6351250x

Demas, G.P., Rabenhorst, M.C., 2001. Factors of subaqueous soil formation: a system of quantitative pedology for submersed environments. Geoderma 102, 189–204. https://doi.org/10.1016/S0016-7061(00)00111-7

Du, B., et al., 2014. Climatic Control on Plant and Soil $\delta^{13}C$ along an Altitudinal Transect of Lushan Mountain in Subtropical China: Characteristics and Interpretation of Soil Carbon Dynamics. PLoS ONE 9(1), e86440. https://doi.org/10.1371/journal.pone.0086440

Erich, E., et al., 2010. Subaqueous soils: their genesis and importance in ecosystem management. Soil Use and Management 26, 245–252. https://doi.org/10.1111/j.1475-2743.2010.00278.x

Everett, M.E., 2013. Near-Surface Applied Geophysics. Cambridge University Press.

Evin, M., 1987. Lithology and fracturing control of rock glaciers in southwestern Alps of France and Italy. In: Giardino, J.R., Shroder Jr. J.F., Vitek, J.D. (Eds.), Rock Glaciers. Allen and Unwin, London, 83–106.

Fan, J., et al., 2017. Carbon and nitrogen signatures of sedimentary organic matter from Dali Lake in Inner Mongolia: Implications for Holocene hydrological and ecological variations in the East Asian summer monsoon margin. Quaternary International 452, 65–78. https://doi.org/10.1016/j.quaint.2016.09.050

Fegel, T.S., et al., 2016. The differing biogeochemical and microbial signatures of glaciers and rock glaciers. Journal of Geophysical Research: Biogeosciences 121(3), 919–932. https://doi.org/10.1002/2015JG003236

Ferronato, C., et al., 2015. Heavy metals risk assessment after oxidation of dredged sediments through speciation and availability studies in the Reno river basin, Northern Italy. Journal of Soil and Sediments 15(5), 1235–1245. https://doi.org/10.1007/s11368-015-1096-4

Fratianni, S., Acquaotta, F., 2017. The Climate of Italy. In: Landscapes and Landforms of Italy. World Geomorphological Landscapes 1, 29–38, Springer International Publishing. https://doi.org/10.1007/978-3-319-26194-2_4

Freppaz, M., et al., 2019. Climatic and pedoclimatic factors driving C and N dynamics in soil and surface water in the alpine tundra (NW-Italian Alps). Nature Conservation 34, 67–90. https://doi.org/10.3897/natureconservation.34.30737

Gardner, J.S., Bajewsky, I., 1987. Hilda rock glacier stream discharge and sediment load characteristics, Sunwapta Pass area, Canadian Rocky Mountains. In: Giardino, J.R., Shroder Jr. J.F., Vitek, J.D. (Eds.), Rock Glaciers. Allen and Unwin, London, 161–174.

Gärtner-Roer, I., 2012. Sediment transfer rates of two active rockglaciers in the Swiss Alps. Geomorphology 167–168, 45–50. https://doi.org/10.1016/j.geomorph.2012.04.013

Gee, G.W., Bauder, J.W., 1986. Methods of soil analysis: part 1 - physical and mineralogical methods. SSSA book series. Soil Science Society of America, American Society of Agronomy.

Giaccone, E., et al., 2015. Climate variations in a high altitude Alpine basin and their effects on a glacial environment (Italian Western Alps). Atmósfera 28(2), 117–128. https://doi.org/10.1016/S0187-6236(15)30004-7

Genereux, D., 1998. Quantifying uncertainty in tracer-based hydrograph separations. Water Resources Research 34(4), 915–919. https://doi.org/10.1029/98WR00010

Giardino, J.R., et al., 1987. Rock Glaciers. Allen and Unwin, London.

Gobbi, M., et al., 2014. Physical and biological features of an active rock glacier of the Italian Alps. The Holocene 24, 1624–1631. https://doi.org/10.1177/0959683614544050

Goodyear, K.L., McNeill, S., 1999. Bioaccumulation of heavy metals by aquatic macro-invertebrates of different feeding guilds: a review. Science of the Total Environment 229, 1–19. https://doi.org/10.1016/S0048-9697(99)00051-0

Gubler, S., et al., 2011. Scale-dependent measurement and analysis of ground surface temperature variability in alpine terrain. The Cryosphere 5(2), 431–443. https://doi.org/10.5194/tc-5-431-2011

Haag, I., et al., 2000. Assessing in-stream erosion and contaminant transport using the end-member mixing analysis (EMMA). The Role of Erosion and Sediment Transport in Nutrient and Contaminant Transfer. IAHS Publ. no 263.

Haeberli, W., et al., 2006. Permafrost creep and rock glacier dynamics. Permafrost and Periglacial Processes 17, 189–214. https://doi.org/10.1002/ppp.561

Hamerlík, L., et al., 2014. Local, among-site, and regional diversity patterns of benthic macroinvertebrates in high altitude waterbodies: Do ponds differ from lakes? Hydrobiologia 723(1), 41–52. https://doi.org/10.1007/s10750-013-1621-7

Harris, H., et al., 2009. Permafrost and climate in Europe: monitoring and modelling thermal, geomorphological and geotechnical responses. Earth-Science Reviews 92, 117–171. https://doi.org/10.1016/j.earscirev.2008.12.002

Harris, S., Pedersen, D., 1998. Thermal regimes beneath coarse blocky materials. Permafrost and Periglacial Processes 9, 107–120. https://doi.org/10.1002/(SICI)1099-1530(199804/06)9:2<107::AID-PPP277>3.0.CO;2-G

Harwart, S., et al., 1999. Lithological and biochemical properties in sediments of Lama Lake as indicators for the late Pleistocene and Holocene ecosystem development of the southern Taymyr Peninsula, Central Siberia. Boreas 28, 167–180. https://doi.org/10.1111/j.1502-3885.1999.tb00212.x

Hauck, C., 2013. New Concepts in Geophysical Surveying and Data Interpretation for Permafrost Terrain. Permafrost and Periglacial Processes 24, 131–137. https://doi.org/10.1002/ppp.1774

Hauck, C., et al., 2003. Using DC resistivity tomography to detect and characterize mountain permafrost. Geophysical Prospecting 51, 273–284. https://doi.org/10.1046/j.1365-2478.2003.00375.x

Hoelzle, M., et al., 1999. Miniature temperature dataloggers for mapping and monitoring of permafrost in high mountain areas: First experience from the Swiss Alps. Permafrost and Periglacial Processes 10, 113–124. https://doi.org/10.1002/(SICI)1099-1530(199904/06)10:2<113::AID-PPP317>3.0.CO;2-A

Hseu, Z.-Y., et al., 2018. Geochemical fractionation of chromium and nickel in serpentine soil profiles along a temperate to tropical climate gradient. Geoderma 327, 97–106. https://doi.org/10.1016/j.geoderma.2018.04.030

Ilyashuk, B.P., et al., 2014. Rock glacier outflows may adversely affect lakes: Lessons from the past and present of two neighboring water bodies in a crystalline-rock watershed. Environmental Science & Technology 48(11), 6192–6200. https://doi.org/10.1021/es500180c

Ilyashuk, B.P., et al., 2018. Rock glaciers in crystalline catchments: hidden permafrost-related threats to alpine headwater lakes. Global Change Biology 24(4), 1548–1562. https://doi.org/10.1111/gcb.13985

IUSS Working Group WRB, 2015. World Reference Base for Soil Resources 2014, update 2015. International soil classification system for naming soils and creating legends for soil maps. World Soil Resources Reports 106, FAO, Rome.

Jones, D.B., et al., 2018. The distribution and hydrological significance of rock glaciers in the Nepalese Himalaya. Global and Planetary Change 160, 123–142. https://doi.org/10.1016/j.gloplacha.2017.11.005

Jones, D.B., et al., 2019. Rock glaciers and mountain hydrology: A review. Earth-Science Reviews 193, 66–90. https://doi.org/10.1016/j.earscirev.2019.04.001

Kandji, E.H.B., et al., 2017. Kinetic testing to evaluate the mineral carbonation and metal leaching potential of ultramafic tailings: case study of the Dumont nickel project, Amos, Québec. Applied Geochemistry 84, 262–276. https://doi.org/10.1016/j.apgeochem.2017.07.005

Kääb, A., Reichmuth, T., 2005. Advance mechanisms of rock glaciers. Permafrost and Periglacial Processes 16, 187–193. https://doi.org/10.1002/ppp.507

Körner, C., 2003. Alpine Plant Life: Functional Plant Ecology of High Mountain Ecosystems. Second Edition, Springer-Verlag Berlin and Heidelberg GmbH & Co. KG, Berlin, Germany.

Krainer, K., Mostler, W., 2002. Hydrology of active rock glaciers: examples from the Austrian Alps. Arctic, Antarctic, and Alpine Research 34(2), 142–149. https://doi.org/10.1080/15230430.2002.12003478

Kristensen, E., Rabenhorst, M.C., 2015. Do marine rooted plants grow in sediment or soil? A critical appraisal on definitions, methodology and communication. Earth-Science Reviews 145, 1–8. https://doi.org/10.1016/j.earscirev.2015.02.005

Kummert, M., Delaloye, R., 2018a. Mapping and quantifying sediment transfer between the front of rapidly moving rock glaciers and torrential gullies. Geomorphology 309, 60–76. https://doi.org/10.1016/j.geomorph.2018.02.021

Kummert, M., Delaloye, R., 2018b. Regional-scale inventory of periglacial moving landforms connected to the torrential network system. Geographica Helvetica 73, 357–371. https://doi.org/10.5194/gh-73-357-2018

Kummert, M., et al., 2018. Erosion and sediment transfer at the front of rapidly moving rock glaciers: observations from the western Swiss Alps. Permafrost and Periglacial Processes 29, 21–33. https://doi.org/10.1002/ppp.1960

LaBrecque, D.J., et al., 1996. The effects of noise on Occam's inversion of resistivity tomography data. Geophysics 61, 538−548. https://doi.org/10.1190/1.1443980

Lee, B.-G., et al., 2000. Influences of dietary uptake and reactive sulfides on metal bioavailability from aquatic sediments. Science 287, 282−284. https://doi.org/10.1126/science.287.5451.282

Loeppert, R.H., Suarez, D.L., 1996. Carbonate and Gypsum. In: Sparks, D.L. (Ed.), Method of Soil Analysis. Part 3, Chemical Methods. SSSA and ASA, Madison, 437–533.

Löv, Å, et al., 2017. Solubility and transport of Cr(III) in a historically contaminated soil - Evidence of a rapidly reacting dimeric Cr(III) organic matter complex. Chemosphere 189, 709–716. https://doi.org/10.1016/j.chemosphere.2017.09.088

MacDonald, D.D., et al., 2000. Development and Evaluation of Consensus-Based Sediment Quality Guidelines for Freshwater Ecosystems. Archives of Environmental Contamination and Toxicology 39, 20–31. https://doi.org/10.1007/s002440010075

Mandal, B.K., et al., 2011. Speciation of Chromium in Soil and Sludge in the Surrounding Tannery Region, Ranipet, Tamil Nadu. ISRN Toxicology. https://doi.org/10.5402/2011/697980

Mania, I., et al., 2019. Prokaryotic diversity and distribution in different habitats of an alpine rock glacier-pond system. Environmental Microbiology 78(1), 70–84. https://doi.org/10.1007/s00248-018-1272-3

McVey, S., et al., 2012. Subaqueous soils (SAS) description. Field book for describing and sampling soils. USDA, Natural Resources Conservation Service, National Soil Survey Center, Lincoln, NE.

Moog, O. (Ed.), (1995). Fauna Aquatica Austriaca, Version 1995. - Wasserwirtschafis-kataster, Bundesministerium für Land- und Forstwirtschaft, Wien.

Morelli, G., LaBrecque, D.J, 1996. Advances in ERT inverse modeling. European Journal of Environmental and Engineering Geophysics 1, 171–186.

Penna, D., (Ilja) van Meerveld, H.J., 2019. Spatial variability in the isotopic composition of water in small catchments and its effect on hydrograph separation. Wiley Interdisciplinary Reviews: Water 6(5), https://doi.org/10.1002/wat2.1367

Peterson, B.J., Howarth, R.W., 1987. Sulfur, carbon, and nitrogen isotopes used to trace organic flow in the salt-marsh estuaries of Sapelo Island, Georgia. Limnology and Oceanography 32, 1195–1213. https://doi.org/10.4319/lo.1987.32.6.1195

Putnam, A.E., Putnam, D.E., 2009. Inactive and relict rock glaciers of the Deboullie Lakes Ecological Reserve, northern Maine, USA. Journal of Quaternary Science 24, 773–784. https://doi.org/10.1002/jqs.1252

Rainbow, P.S., 2002. Trace metal concentrations in aquatic invertebrates: why and so what? Environmental Pollution 120, 497–507. https://doi.org/10.1016/S0269-7491(02)00238-5

Ribolini, A., Fabre, D., 2006. Permafrost existence in the rock glaciers of the Argentera Massif (Maritime Alps, Italy). Permafrost and Periglacial Processes 17, 49–63. https://doi.org/10.1002/ppp.548

Ribolini, A., et al., 2007. Relationships between glacier and rock glacier in the Maritime Alps, Schiantala Valley, Italy. Quaternary Research 68, 353–363. https://doi.org/10.1016/j.yqres.2007.08.004

Ribolini, A., et al., 2010. The internal structure of rock glaciers and recently-deglaciated slopes as revealed by geoelectrical tomography: insights on permafrost and recent glacial evolution in the Central and Western Alps (Italy-France). Quaternary Sciences Reviews 29, 507–521. https://doi.org/10.1016/j.quascirev.2009.10.008

Salerno, F., et al., 2014. High alpine ponds shift upwards as average temperatures increase: A case study of the Ortles-Cevedale mountain group (Southern Alps, Italy) over the last 50 years. Global and Planetary Change 120, 81–91. https://doi.org/10.1016/j.gloplacha.2014.06.003

Schoeneberger, P., et al., 2012. Field book for describing and sampling soils, version 3.0. Natural Resources Conservation Service, National Soil Survey Center, Lincoln, NE, USA.

Scotti, R., et al., 2013. A regional inventory of rock glaciers and protalus ramparts in the central Italian Alps. Geomorphology 186, 136–149. https://doi.org/10.1016/j.geomorph.2012.12.028

Seppi, R., et al., 2015. Current transition from glacial to periglacial processes in the Dolomites (South-Eastern Alps). Geomorphology 228, 71–86. https://doi.org/10.1016/j.geomorph.2014.08.025

Soil Survey Staff, 2014. Keys to Soil Taxonomy. 12th ed., United States Department of Agriculture, Natural Resources Conservation Service.

Sorg, A, et al., 2015. Contrasting responses of central Asian rock glaciers to global warming. Scientific Reports 5, 8228. https://doi.org/10.1038/srep08228

Stanchi, S., et al., 2015. Soil aggregation, erodibility, and erosion rates in mountain soils (NWAlps, Italy). Solid Earth 6, 403–414. https://doi.org/10.5194/se-6-403-2015

Talbot, M.R., Lærdal, T., 2000. The Late Pleistocene-Holocene palaeolimnology of Lake Victoria, East Africa, based upon elemental and isotopic analyses of sedimentary organic matter. Journal of Paleolimnology 23, 141–164. https://doi.org/10.1023/A:1008029400463

Tampucci, D., et al., 2017. Ecology of active rock glaciers and surrounding landforms: climate, soil, plants and arthropods. Boreas 46, 185–198. https://doi.org/10.1111/bor.12219

Teranes, J.L., Bernasconi, S.M., 2005. Factors controlling $\delta^{13}C$ values of sedimentary carbon in hypertrophic Baldeggersee Switzerland, and implications for interpreting isotope excursions in lake sedimentary records. Limnology and Oceanography 50, 914–922. https://doi.org/10.4319/lo.2005.50.3.0914

Thevenon, F., et al., 2012. Elemental (C/N ratios) and isotopic (δ^{15}Norg, δ^{13}Corg) compositions of sedimentary organic matter from a high-altitude mountain lake (Meidsee, 2661 m a.s.l., Switzerland): Implications for Lateglacial and Holocene Alpine landscape evolution. The Holocene 22(10), 1135–1142. https://doi.org/10.1177/0959683612441841

Thies, H., et al., 2007. Unexpected response of high Alpine Lake waters to climate warming. Environmental Science & Technology 41, 7424–7429. https://doi.org/10.1021/es0708060

Thies, H., et al., 2013. Evidence of rock glacier melt impacts on water chemistry and diatoms in high mountain streams. Cold Regions Science and Technology 96, 77–85. https://doi.org/10.1016/j.coldregions.2013.06.006

Thies, H., et al., 2018. Peculiar arsenic, copper, nickel, uranium, and yttrium-rich stone coatings in a high mountain stream in the Austrian Alps. Austrian Journal of Earth Sciences 110(2). doi:10.17738/ajes.2017.0012

Wang, F., et al., 2015. Joint toxicity of sediment-associated DDT and copper to a polychaete, *Nereis succinea*. Ecotoxicology 24, 424–432. https://doi.org/10.1007/s10646-014-1391-7

Wang, Y.M., Wooller, M.J., 2006. The stable isotopic (C and N) composition of modern plants and lichens from northern Iceland: with ecological and paleoenvironmental implications. Jökull 56, 27–37.

Watanabe, K., et al., 2008. Biodilution of heavy metals in a stream macroinvertebrate food web: evidence from stable isotope analysis. Science of The Total Environment 394, 57–67. https://doi.org/10.1016/j.scitotenv.2008.01.006

White, W.M., 2015. Isotope Geochemistry. John Wiley & Sons Inc., New York, United States.

Williams, M.W., et al., 2006. Geochemistry and source waters of rock glacier outflow, Colorado Front Range. Permafrost and Periglacial Processes 17(1), 13–33. https://doi.org/10.1002/ppp.535

Williams, M.W., et al., 2007. Nitrate content and potential microbial signature of rock glacier outflow, Colorado Front Range. Earth Surface Processes and Landforms 32, 1032–1047. https://doi.org/10.1002/esp.1455

Wischmeier, W.H., Mannering, J.W., 1969. Relation of Soil Properties to its Erodibility. Soil Science Society of America Journal Abstract 33(1), 131–137.

Zemp, M., et al., 2015. Historically unprecedented global glacier decline in the early 21st century. Journal of Glaciology 61(228), 745–762. https://doi.org/10.3189/2015JoG15J017

Figures

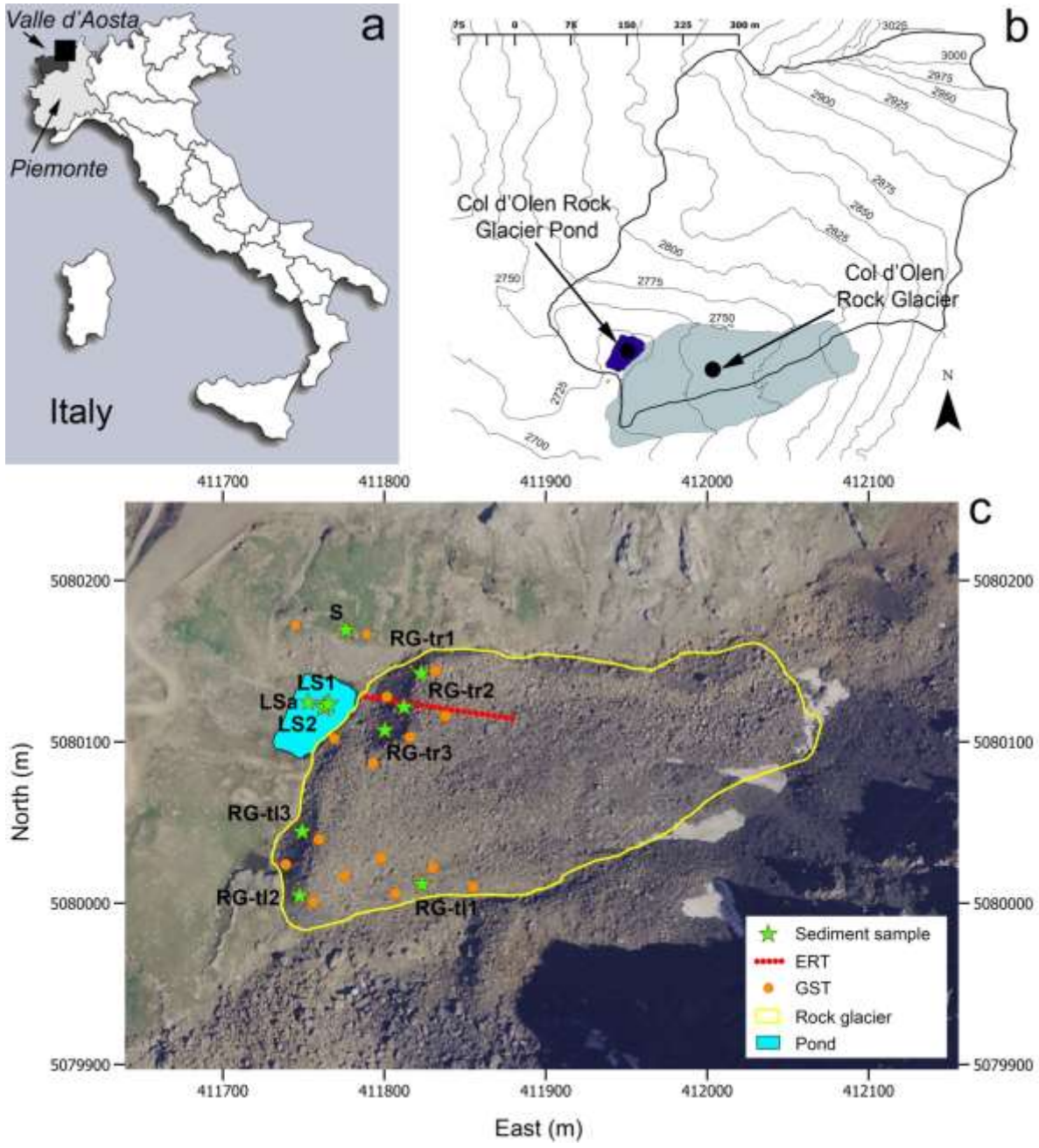

Figure 1 - (a) Location of the study area in Italy. (b) Elevation map of the study area showing the extent of the catchment, the Col d'Olen Rock Glacier and the Col d'Olen Rock Glacier Pond. (c) Locations of sediment sampling sites, ground surface temperature (GST) sensors, and electrical resistivity tomography (ERT) survey line. Sampling points: LS (Lacustrine Sediment); S (Soil); RG-tr (Rock Glacier sediment-tongue right); RG-tl (Rock Glacier sediment-tongue left). Aerial image year 2006, coordinate system WGS 84 / UTM zone 32N.

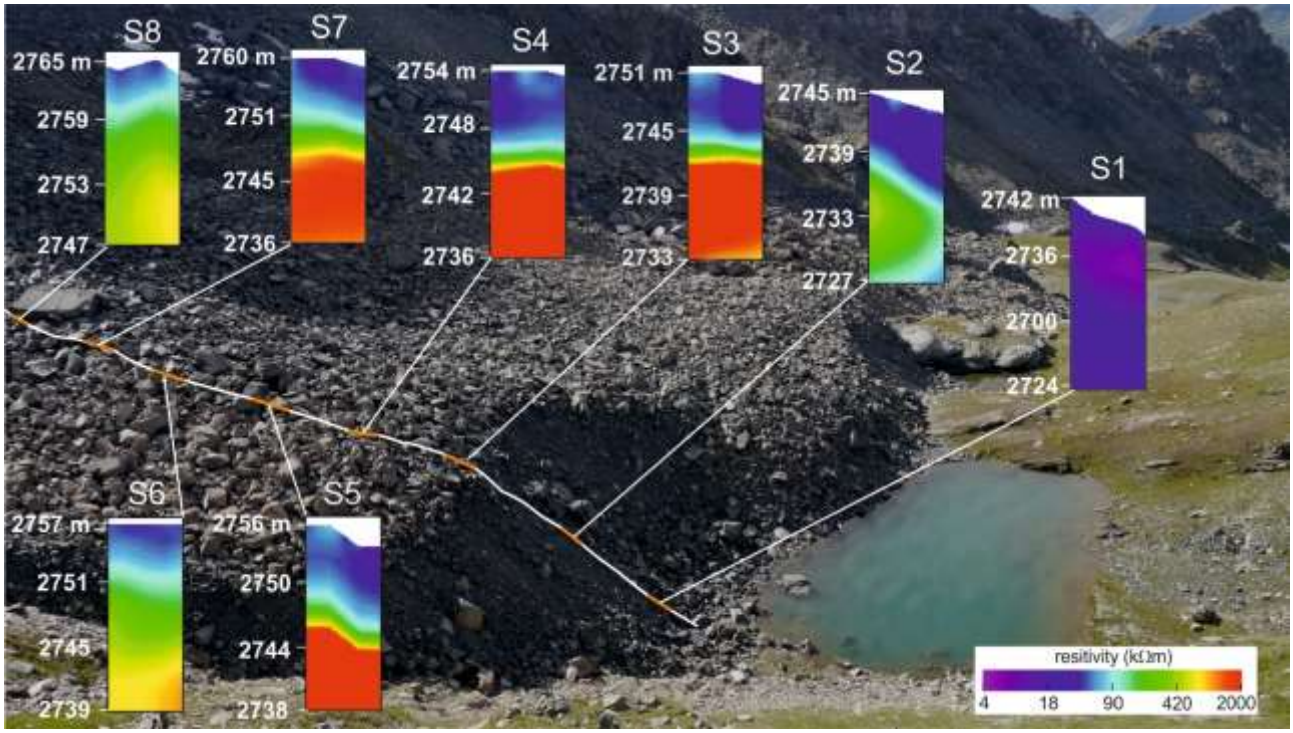

Figure 2 - Vertical sections extracted from the geoelectrical resistivity tomography along RG-tr. The location of the tomography is reported in Fig. 1c.

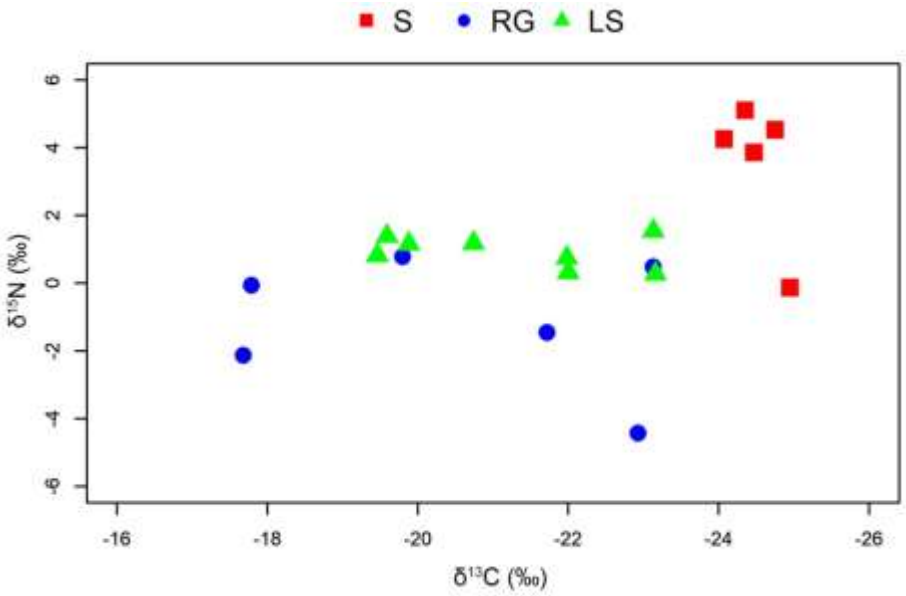

Figure 3 - Scatter plot of $\delta^{13}C$ vs. $\delta^{15}N$ for all soil and sediment samples in Soil (S), Rock Glacier (RG), and Lacustrine Sediment (LS) sampling sites.

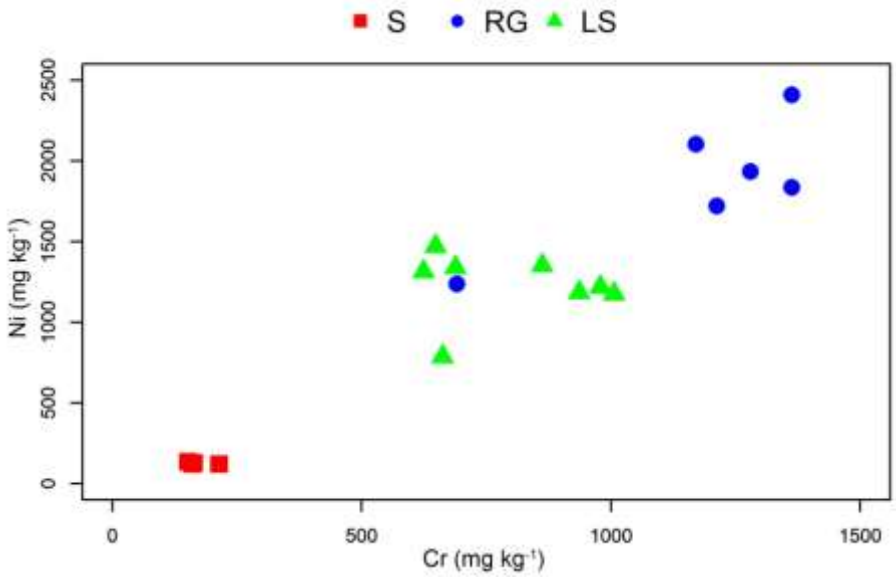

Figure 4 - Scatter plot of Cr vs. Ni for all soil and sediment samples in Soil (S), Rock Glacier (RG), and Lacustrine Sediment (LS) sampling sites.

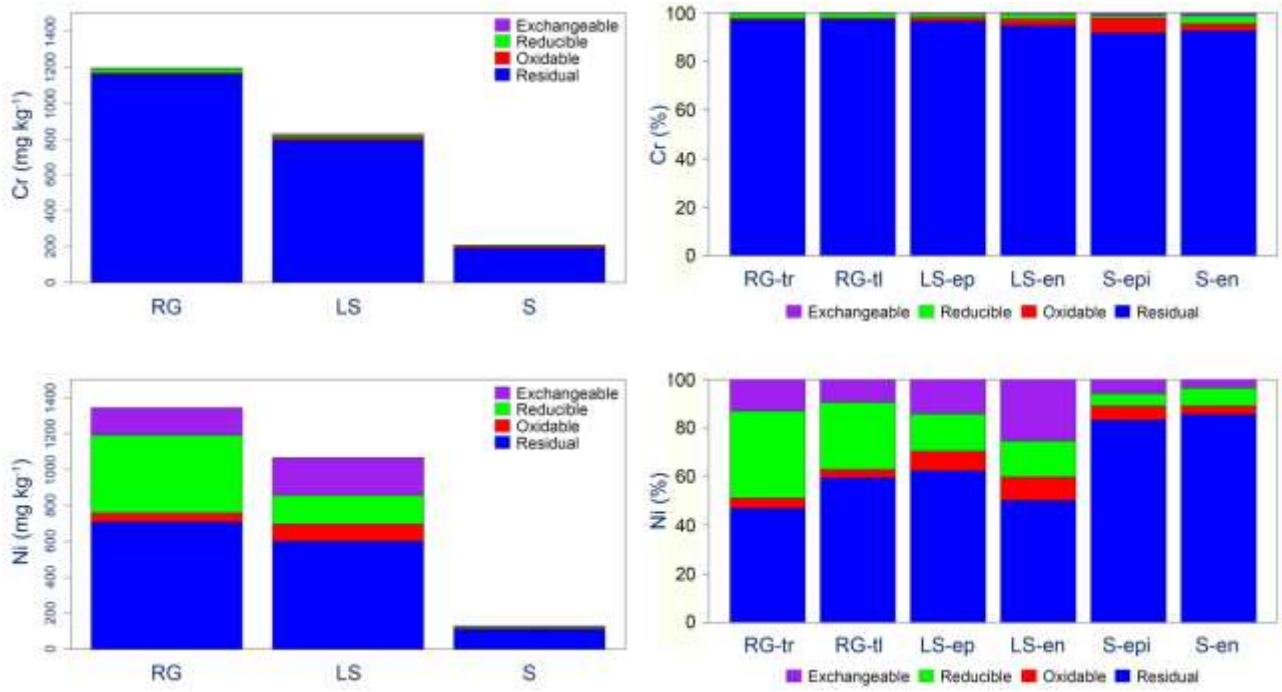

Figure 5 - Left: sequential extraction of Cr and Ni in Soil (S), Lacustrine Sediment (LS), and Rock Glacier (RG) (left) (average values for each sampling site). Right: sequential extraction of Cr and Ni in Rock Glacier (RG) sediments (tongue right, RG-tr and left, RG-tl), Lacustrine Sediment epipedon (LS-ep) and endopedon (LS-en), and Soil epipedon (S-ep) and endopedon (S-en).

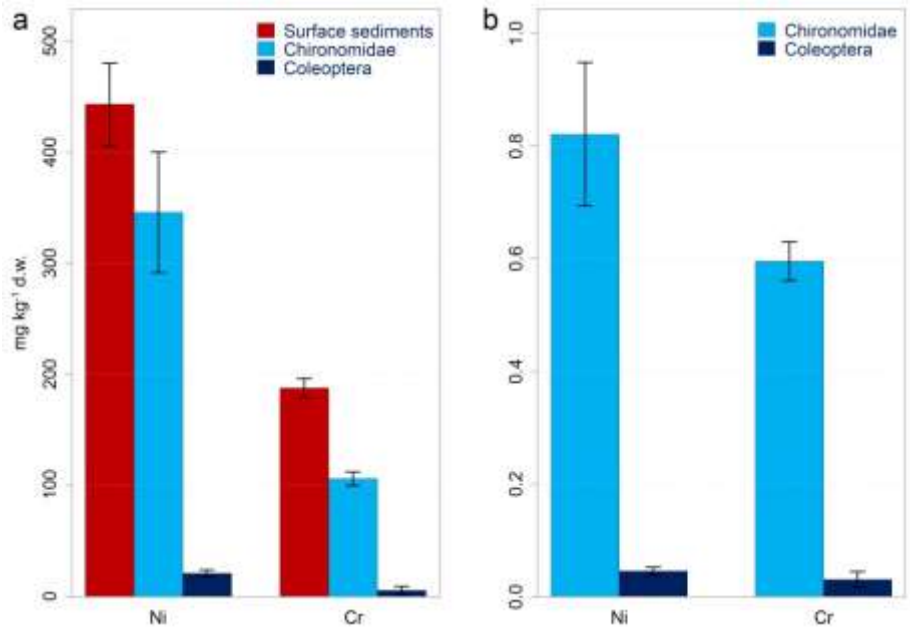

Figure 6 - a) Concentrations of key trace metals in surface lacustrine sediments (LSa sampling site) and in two benthic invertebrate taxa collected in the pond. b) Values of Biota-Sediment Concentrations Factors (BSAF) for both taxa. Columns represent mean values, bars ± standard deviation (n = 3 for sediments, n = 2 for organisms and BSAF).

Tables

Sampling location	MAGST (°C)	GFI (°C·day)	WEqT (°C)
Rock Glacier tongue right (RG-tr)	–0.1 ± 0.4	–748 ± 128	−4.3 ± 1.7
Rock Glacier tongue left (RG-tl)	0.6 ± 0.5	–540 ± 137	−3.1 ± 1.1
Soil (S)	2.5 ± 0.5	–6 ± 5	0.1 ± 0.1

Table 1 - Thermal regime of the ground surface on the rock-glacier tongues and in the surrounding soil. MAGST: mean annual ground surface temperature; GFI: ground freezing index (annual mean); WEqT: winter equilibrium temperature (annual mean). Mean value of the sensors for each measurement area ± standard deviation are reported.

		Sand	Silt	Clay	pH	EC	SOC	SON	C/N	$\delta^{13}C$	$\delta^{15}N$
		%	%	%		µS cm^{-1}	g kg^{-1}	g kg^{-1}		‰	‰
RG	**RG-tl**	76.4 ± 8.6	19.9 ± 6.8	3.6 ± 1.8	6.7 ± 0.5	57.6 ± 5.5	0.3 ± 0.1	0.02 ± 0.01	12.3 ± 0.4	-22.6 ± 0.8	-1.8 ± 2.5
	RG-tr	78.5 ± 3.2	18.0 ± 4.8	3.5 ± 1.7	6.6 ± 0.4	65.6 ± 14.0	0.4 ± 0.3	0.03 ± 0.02	14.7 ± 0.6	-18.4 ± 1.2	-0.5 ± 1.5
LS	**LS-ep**	11.0 ± 1.6	82.8 ± 1.1	6.1 ± 2.4	5.2 ± 0.3	347 ± 182	1.3 ± 0.1	0.1 ± 0.0	10.0 ± 0.1	-22 ± 1.0	0.6 ± 0.4
	LS-en	17.0 ± 11.1	76.3 ± 10.3	6.8 ± 2.4	5.2 ± 0.2	369 ± 56.4	2.0 ± 0.4	0.2 ± 0.0	10.2 ± 0.8	-20.5 ± 1.8	1.2 ± 0.3
S	**S-ep**	53.0 ± 0.0	35.9 ± 6.9	11.1 ± 6.9	4.9 ± 0.2	158 ± 112	6.0 ± 3.0	0.6 ± 0.4	9.5 ± 0.7	-24.7 ± 0.3	1.9 ± 2.8
	S-en	59.4 ± 4.2	33.4 ± 3.9	7.2 ± 0.3	5.1 ± 0.1	25.2 ± 9.2	1.3 ± 0.4	0.1 ± 0.0	11.2 ± 0.3	-24.4 ± 0.3	4.6 ± 0.4

Table 2 - Physicochemical analysis of Rock Glacier (RG) sediments (tongue right, RG-tr and left, RG-tl), Lacustrine Sediment epipedon (LS-ep) and endopedon (LS-en), and Soil epipedon (S-ep) and endopedon (S-en). Mean value ± standard deviation are reported.

		Ca	K	Mg	P	S	Cr	Ni
		g kg^{-1}					mg kg^{-1}	
RG	**RG-tl**	3.8 ± 2.5	1.2 ± 0.9	120 ± 36.5	0.5 ± 0.3	1.0 ± 0.0	1061 ± 322	1630 ± 357
	RG-tr	1.2 ± 0.2	0.6 ± 0.5	143 ± 3.5	0.2 ± 0.0	0.9 ± 0.0	1299 ± 111	2115 ± 287
LS	**LS-ep**	3.5 ± 0.3	4.0 ± 0.5	89.2 ± 3.9	0.5 ± 0.1	0.5 ± 0.1	946 ± 63.1	1233 ± 82.0
	LS-en	4.8 ± 0.5	4.6 ± 0.8	64.5 ± 5.9	0.6 ± 0.0	0.7 ± 0.2	656 ± 26.6	1228 ± 301
S	**S-ep**	9.0 ± 4.4	3.5 ± 1.8	18.6 ± 2.0	0.8 ± 0.0	0.6 ± 0.1	187 ± 38.5	124 ± 5.3
	S-en	7.4 ± 2.6	2.9 ± 0.7	18.4 ± 0.8	0.7 ± 0.2	1.0 ± 0.0	158 ± 6.6	129 ± 6.8

Table 3 - Macro elements and trace metals in Rock Glacier (RG) tongue right (RG-tr) and left (RG-tl), Lacustrine Sediment epipedon (LS-ep) and endopedon (LS-en), and Soil epipedon (S-ep) and endopedon (S-en). Mean value ± standard deviation are reported.

		Ca	K	Mg	P	S	Cr	Ni
		mg kg^{-1}					µg kg^{-1}	
RG	**RG-tl**	14.4 ± 4.4	nd	18.8 ± 3.5	nd	5.3 ± 17.6	nd	2.7 ± 3.6
	RG-tr	9.6 ± 2.8	nd	29.3 ± 3.0	nd	7.3 ± 1.7	nd	3.7 ± 2.1
LS	**LS-ep**	130 ± 2.8	9.5 ± 4.3	95.2 ± 3.1	nd	255 ± 1.8	nd	29.7 ± 1.6
	LS-en	124 ± 3.7	9.0 ± 3.5	76.9 ± 3.4	nd	210 ± 3.2	nd	26.0 ± 1.4
S	**S-ep**	26.1 ± 1.1	36.9 ± 1.0	16.9 ± 1.1	16.2 ± 1.1	28.1 ± 1.7	23.6 ± 0.0	0.3 ± 1.1
	S-en	3.1 ± 6.2	nd	2.4 ± 20.0	nd	3.1 ± 1.6	nd	nd

Table 4 - Soluble macro elements and trace metals in Rock Glacier (RG) tongue right (RG-tr) and left (RG-tl), Lacustrine Sediment epipedon (LS-ep) and endopedon (LS-en), and Soil epipedon (S-ep) and endopedon (S-en). Mean value ± standard deviation are reported; “nd” is not detectable.